Journal of Solid State Chemistry **145,** 253–259 (1999)
Article ID jssc.1999.8259, available online at http://www.idealibrary.com on IDEAL®

# Short-Range Order in Se-Rich Ge–Se Glasses—An Extended X-Ray Absorption Fine Structure Study

Egil Gulbrandsen,*,[1] Hege Britt Johnsen,* Monica Endregaard,*,[2] Tor Grande,† and Svein Stølen*,[3]

*Department of Chemistry, University of Oslo, P. O. Box 1033, N-0315 Oslo, Norway; and †Department of Inorganic Chemistry, The Norwegian University of Science and Technology, N-7034 Trondheim, Norway

Received September 15, 1998; in revised form February 24, 1999; accepted March 10, 1999

**The short-range order in vitreous $Ge_{1-x}Se_x$ ($2/3 \leq x \leq 1$) at 80 K was studied by EXAFS spectroscopy at the Ge and Se K-edges. The results were analyzed using theoretical phase shift and amplitude functions and by comparison to crystalline $GeSe_2$ and Se as model compounds. The $GeSe_4$ tetrahedron is the main structural entity for all the Ge–Se alloys. The results indicate a slight increase in Ge coordination and a decrease in Se coordination with increasing Se content. Possible sources of error are discussed, and possible origins of the structural changes are suggested.** © 1999 Academic Press

*Key Words:* **Ge–Se glasses; short-range order; EXAFS.**

## INTRODUCTION

The structure and properties of amorphous semiconductors like the germanium and silisium chalcogenides have received considerable attention over the last decades. Short-range order (SRO) in these materials is defined in terms of the number of nearest neighbors, the nearest-neighbor bond length, and the bond angle defining the spatial arrangement of the nearest neighbor atoms around each type of central atom. Medium-range order (MRO) refers to the connectivity (e.g., corner, edge, and face sharing) of the basic SRO polyhedra.

Two simple models represent the extremes in the description of SRO in covalent glasses. Whereas the random covalent network model treats the distribution of bonds as purely random, determined by the local coordination numbers and the composition, the chemically ordered network model assumes that a completely short-range ordered structure forms for some stoichiometric composition, e.g., for $GeSe_2$ in the Ge–Se system. The stability of this short-range ordered structure is inferred from the existence of a high-melting crystalline compound, $GeSe_2$, with structure based on 50% corner sharing and 50% edge sharing $GeSe_4$ tetrahedra (1).

Direct structural evidence for a large degree of chemical ordering in the Ge–Se system has been obtained from EXAFS studies. Zhou *et al.* (2) studied amorphous Ge–Se alloys with $0.60 < x_{Se} < 0.80$ and found that the $GeSe_4$ tetrahedra remained stable in this compositional region. The second-neighbor shell was observable at a level only slightly above the noise level. Calculations based on bond angle distribution show that the disorder is largely due to a spread in the bond angle (2). Only two alloys with $x_{Se} > 2/3$ were studied ($x_{Se} = 0.75$ and 0.80).

The Ge atoms in glasses with a Se-content higher than that of those studied by Zhou *et al.* (2) also seem to be tetrahedrally coordinated (3). Spectroscopic studies indicate that there are few Ge–Ge bonds and, furthermore, Ge–Se–Ge sequences remain scarce as long as the Ge concentration in the alloy is low (4).

The MRO of $GeSe_2$ and Ge-rich alloys is more uncertain and several complex models have been proposed, i.e., cluster rings of Ge atoms interconnected through single Se atoms (4) and raft-type structures bordered by Se–Se wrong bonds (5).

Changes in coordination are observed on irradiation with ultraviolet light (6,7). The reversible photostructural changes lead to overcoordination of Ge and under-coordination of Se with respect to the annealed glassy state (formation of Ge with higher coordination and terminal Se). The magnitude of the photostructural change is reported to be larger in off-stoichiometric samples. Raman spectroscopic data indicate that the ratio of edge- to corner-sharing bonds varies on irradiation (8). This effect has not been correlated with the apparent coordination changes observed using EXAFS (6, 7).

In this paper an EXAFS study of the short-range order in Se-rich Ge–Se glasses ($2/3 < x_{Se} < 0.975$) is reported. The

[1] Present address: Institute for Energy Technology, P. O. Box 40, N-2007, Kjeller, Norway.
[2] Present address: Norwegian Defense Research Establishment (FFI), P. O. Box 25, N-2007, Kjeller, Norway.
[3] To whom correspondence should be addressed. Tel: +47-22855601. Telefax: +47-22855441. E-mail: svein.stolen@kjemi.unio.no.



0022-4596/99 $30.00

main objective was to determine the coordination numbers for Ge in Se-rich glasses for which no previous data have been reported by EXAFS spectroscopy.

## EXPERIMENTAL

The syntheses of crystalline compounds and glasses in the Ge–Se system have been described previously (9). The homogeneity and vitreous character of the samples were confirmed by optical microscopy and Raman spectroscopy. Raman spectra of selected samples are shown in Fig. 1.

The samples were diluted and ground with BN, pressed to discs in ~1-mm-thick sample holders, and sealed with Kapton tape. The samples were dimensioned to have an absorption edge step below 1.5 to minimize size effects (10). The EXAFS spectra were measured at liquid $N_2$ temperature using a cryostat to reduce the thermal disorder. Most of the EXAFS spectra (germanium K-edge, 11 103 eV; selenium K-edge, 12 659 eV) were recorded in transmission mode using Ar/He ion chambers at the Synchrotron Radiation Source (SRS), Daresbury Laboratory (2 GeV, with typical current in the range 150–250 mA), station 7.1. In addition some spectra were collected at the National Synchrotron Light Source (NSLS) at Brookhaven National Laboratory (2.6 GeV, with typical current in the range 60–130 mA), beamline X11A and X23A. Energy resolution is 10 eV below the edge, 0.5 eV in the edge region, and $k$ steps of 0.05 $Å^{-1}$ in the EXAFS region, 2–17 $Å^{-1}$. The double-crystal Si(111) monochromator was detuned to reduce unwanted harmonics. The Ge and Se edge results were calibrated using the first maximum in the first derivative of iron foil spectrum (7111.2 eV). The energy calibration was checked by simultaneously registering the spectrum of a Ge foil in a reference ion chamber.

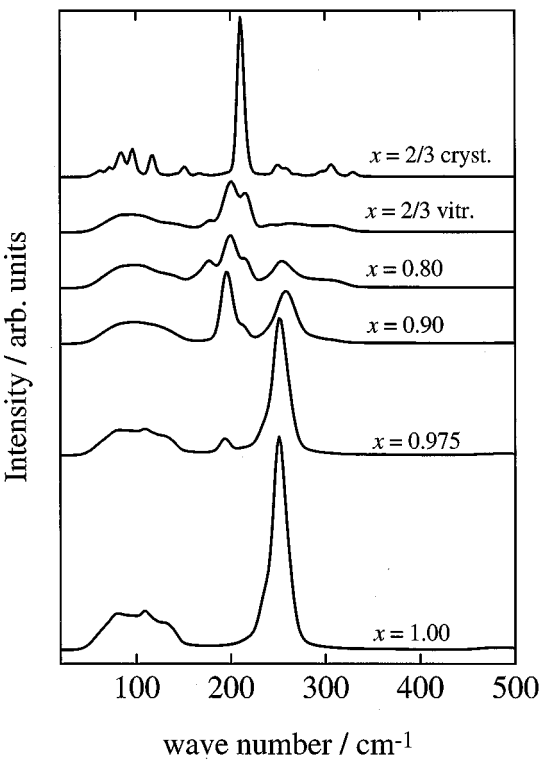


**FIG. 1.** Raman spectra of selected $Ge_{1-x}Se_x$ samples.

## DATA REDUCTION AND ANALYSIS

The EXAFS data reduction and analysis were carried out in a standard manner (11,12) using the Daresbury suite of EXAFS analysis programs: EXCALIB, EXBACK, and EXCURV 92 (13). For each sample, two or three absorption spectra were summed to reduce noise. A linear preedge contribution was subtracted. The postedge absorption was subtracted by fitting two polynomials of third degree in energy in a manner avoiding introduction of high-frequency oscillations in the fitting functions. The resulting EXAFS spectra were edge-step normalized using the absorption at 50 eV above the edge to define the step. The normalized spectra were then corrected for the energy-dependent absorption (*MacMaster corrected*) (11) using the Victoreen functions (11). This correction had negligible effect on the coordination number. This finding is in line with previously reported results (14). The $k^3$-weighted EXAFS data for crystalline and vitreous $GeSe_2$ at the Ge K-edge and the Se K-edge performed at SRS and at NSLS are shown in Fig. 2a. Corresponding data for selected vitreous samples are shown in Figs. 2b and 2c at the Ge K-edge and the Se K-edge, respectively. In the analysis of the EXAFS spectra, $k^3$ and $k$ weighting was used. The spectra were Fourier transformed in the $k$ range between 2.0 and 17.0 $Å^{-1}$ for the Ge K-edge spectra and between 2.0 and 16.0 $Å^{-1}$ for the Se K-edge spectra. As examples, phase shift-corrected Fourier transforms of the $k^3$-weighted data for crystalline and vitreous $GeSe_2$ at the Ge K-edge, as well as for crystalline Se (space group $P3_121$, $N = 2.0$, $R = 2.329$ Å (15)) and for vitreous Se at the Se K-edge are shown in Fig. 3. The second shell is observed for crystalline $GeSe_2$ but not for vitreous $GeSe_2$. Also for the other vitreous samples, only the first shell was observed and the glasses preserve short-range order primarily to the first shell. In the present paper, we focus on the first shell data analysis. To isolate the first shell EXAFS, the first shell peak of the Fourier transform was inversely transformed through a Gaussian window function (13). The extension of the window function for the vitreous samples is from 1.5 to 2.7 Å for Ge K-edge and from 1.5 to 2.6 Å for Se K-edge. For crystalline $GeSe_2$ a somewhat larger distance space, 1.5 to 4.0 Å, was used to allow for the second shell. The EXAFS signal range

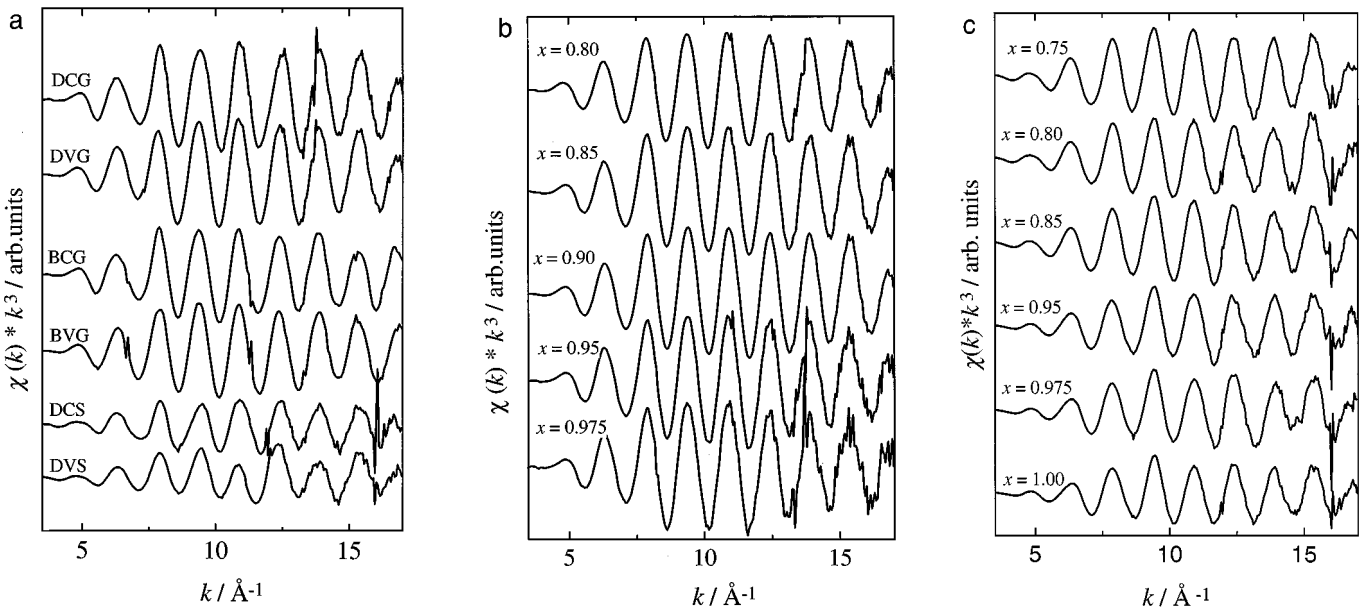


**FIG. 2.** $k^3$-weighted EXAFS data for (a) crystalline and vitreous $GeSe_2$ at the Ge K-edge and the Se K-edge (D, Daresbury (SRS); B, Brookhaven (NSLS); C, crystalline; V, vitreous; G, Ge K-edge; S, Se K-edge); (b) selected vitreous $Ge_{1-x}Se_x$ samples at the Ge K-edge; (c) selected vitreous $Ge_{1-x}Se_x$ samples at the Se K-edge.

utilized for analysis was somewhat smaller than the Fourier transformed range: 3.5 to 16 $Å^{-1}$ for the Ge–edge and 3.5 to 15 $Å^{-1}$ for the Se edge. This was done to minimize the error introduced by Fourier filtering (14). The EXAFS spectra were analyzed with the curved-wave, single-scattering theory (16, 17) of EXCURV92. Theoretical phase shift and amplitude functions were calculated using XALFA ground state and exchange potentials (13). Spectra of the model compounds, crystalline $GeSe_2$ and Se, were used to determine the amplitude reduction factors. The results obtained were 0.79 and 0.78, respectively, for $GeSe_2$ and Se.

Ge and Se with atomic numbers 32 and 34 have similar atomic sizes and thus lead to similar heteropolar and homopolar bond distances. Furthermore backscattering amplitudes and phase shifts of Ge and Se are also of the same order and lead to increased difficulty in the data analysis. It is thus difficult to resolve Se and Ge as nearest neighbors to a central atom and a complete short-range order is assumed; i.e., each Ge atom is surrounded by Se atoms only.

In the analysis of the EXAFS spectra the following variables were treated as refinable: the energy-zero reference parameter $E_0$, the distance $r_j$ between the atoms in shell j and the X-ray absorbing atom; the number of atoms $N_j$ in shell j, and the Debye-Waller factor $2\sigma_j^2$ for shell j. $k^3$ and $k^1$ weighting were used to obtain consistent sets of values for the correlated quantities $r_j$ and $E_0$ and $N_j$ and $2\sigma_j^2$ (18).

## RESULTS

The Raman data presented in Fig. 1 are in good accord with earlier reported data (3,8). The dominant line for Se at 250 $cm^{-1}$ is assigned to $A_1$ and $E_2$ modes of $Se_8$ rings and the shoulder at 235 $cm^{-1}$ is due to $A_1$ and E modes of the Se–Se chain. The intensity of these lines decreases with increasing Ge content. For vitreous $GeSe_2$ the double peak at 200 and 215 $cm^{-1}$ is due to vibrational modes for the main building block, the $GeSe_4$ tetrahedras. The intense 200-$cm^{-1}$ band is assigned to the symmetric breathing vibrational mode of the corner-shared $GeSe_4$ tetrahedra, while the weaker band at 215 $cm^{-1}$ is due to the quasi-localized breathing mode on the edge-sharing $Ge_2Se_8$ tetrahedra. The corresponding bands in crystalline $GeSe_2$ are observed at 211 (very intense) and 216 (week) $cm^{-1}$, respectively. The presence of a week line in this frequency region for $x = 0.975$ indicates that $GeSe_4$ tetrahedras are present also in glasses with very low Ge content.

Typical observed and calculated first shell EXAFS spectra are shown in Fig. 4. Ge K-edge data for vitreous $GeSe_2$ and $Ge_{0.05}Se_{0.95}$ and Se K-edge data for crystalline and vitreous Se are given. The observed and calculated spectra are generally in good agreement. The deduced structural data for the first coordination spheres for the Ge and Se K-edges are given in Fig. 5. The coordination number, the interatomic distance, and the Debye–Waller factor are

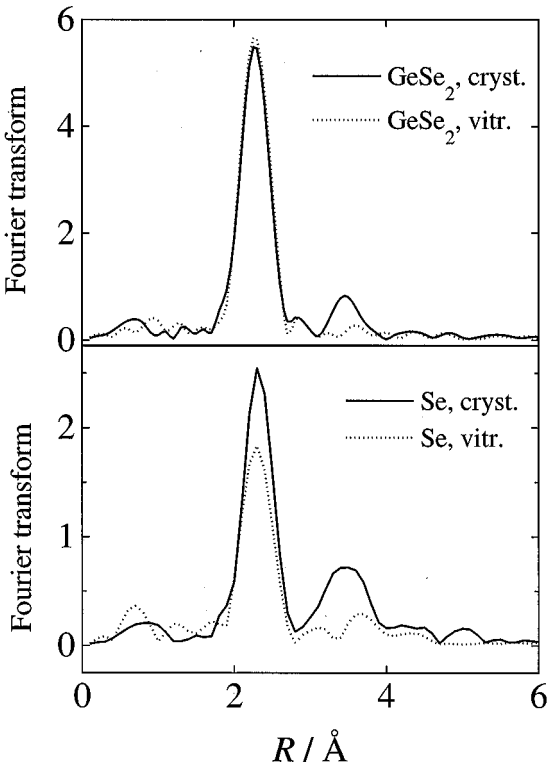


**FIG. 3.** Phase shift-corrected Fourier transforms of the $k^3$-weighted EXAFS spectra for crystalline and vitreous $GeSe_2$ at the Ge K-edge (top) and for crystalline and vitreous Se at the Se K-edge (bottom).

shown as a function of composition. Earlier results reported by Zhou *et al.* (2) and by Peyroutou *et al.* (19, 20) are included for comparison.

*Germanium K-edge.* Germanium is expected to be four-coordinated in the compositional range studied. A weak increase in the coordination number with increasing Se content is, however, deduced. The nearest-neighbor distances and the Debye–Waller factor also increase slightly with Se content from 2.348 Å and 0.0033 $Å^2$ for vitreous $GeSe_2$ to 2.357 Å and 0.0049 $Å^2$ for $Ge_{0.025}Se_{0.975}$. The results from NSLS give interatomic distance and Debye–Waller factor values somewhat larger than those obtained from the SRS experiments. The shortest Ge–Se bond length for amorphous $GeSe_2$ is in good agreement with literature values for crystalline $GeSe_2$.

The present results are in general agreement with those reported for alloys with $2/3 < x_{Se} < 0.80$ by Zhou *et al.* (2). The shortest Ge–Se bond length reported by Zhou *et al.* (2) for glassy $GeSe_2$ is, however, slightly long compared to that in the crystal and that reported in the present work. EXAFS data of Ge–Se alloys have also been reported by Peyroutou *et al.* (19, 20). No raw data were shown; hence, the quality of these data are uncertain. In contrast to Zhou *et al.* (2), Peyroutou *et al.* (19, 20) were able to resolve both the first and the second coordination sphere for their vitreous samples. The Debye–Waller factors reported are anomalously low.

*Selenium K-edge.* The Se coordination and the shortest interatomic distance for pure Se are apparently different in the vitreous and crystalline states: 2.0 and 2.374 Å were observed for the crystalline phase; ~1.5 and ~2.34 Å were observed for vitreous Se. The short-range order in the vitreous state does not seem to be affected by the preparation route, as samples obtained by melt quenching from different temperatures as well as by physical vapor deposition gave similar results. Low coordination numbers and interatomic distances were also observed for the most Se-rich alloys. Se is found to be two-coordinated in crystalline and vitreous $GeSe_2$ and in the more Se-poor vitreous alloys, and the shortest Se–Se distance is equal in crystalline and vitreous $GeSe_2$.

Also at this edge, the present results are in general agreement with those reported by Zhou *et al.* for $2/3 < x_{Se} < 0.80$ (2). The coordination number obtained by Zhou *et al.* (2) for vitreous Se, $1.8 \pm 0.2$, is larger than that obtained in the present study. Low coordination numbers for Se were observed by Peyroutou *et al.* (19, 20).

The low coordination number presently obtained suggests that the average chain length in vitreous Se is four. This is at variance with previously published estimates of the average chain length, although the chain length is reported to decrease with increasing temperature. The average chain length at 1823 K, as deduced by NMR spectroscopy, is seven (21). A recent first principles molecular dynamics simulation suggests even shorter chain lengths and calculates the coordination numbers at 870, 1170, and 1770 K to be 1.9, 1.7, and 1.5. The simulation also indicates that the interatomic bond length decreases with increasing temperature (22).

## DISCUSSION

Silisium and germanium chalcogenide glasses are generally believed to have a well-defined short-range order. Thus, the $GeSe_4$ tetrahedra is expected to be the main structural building block for all compositions of glassy $Ge_{1-x}Se_x$ (with $2/3 < x < 1$). Even though this is compatible with the present experiments, our results also indicate that a change in coordination with composition is possible. A slight overcoordination of Ge and undercoordination of Se are deduced for the most Se-rich samples. Similar observations were observed by Gladden *et al.* on band-gap illumination of a $GeSe_2$ glass (6, 7). Gladden showed that the coordination changes were reversible (6, 7). By annealing at around the glass transition temperature the structure reverted to the normal 4:2 coordination. Although the presently obtained Ge coordination number apparently increases with mole

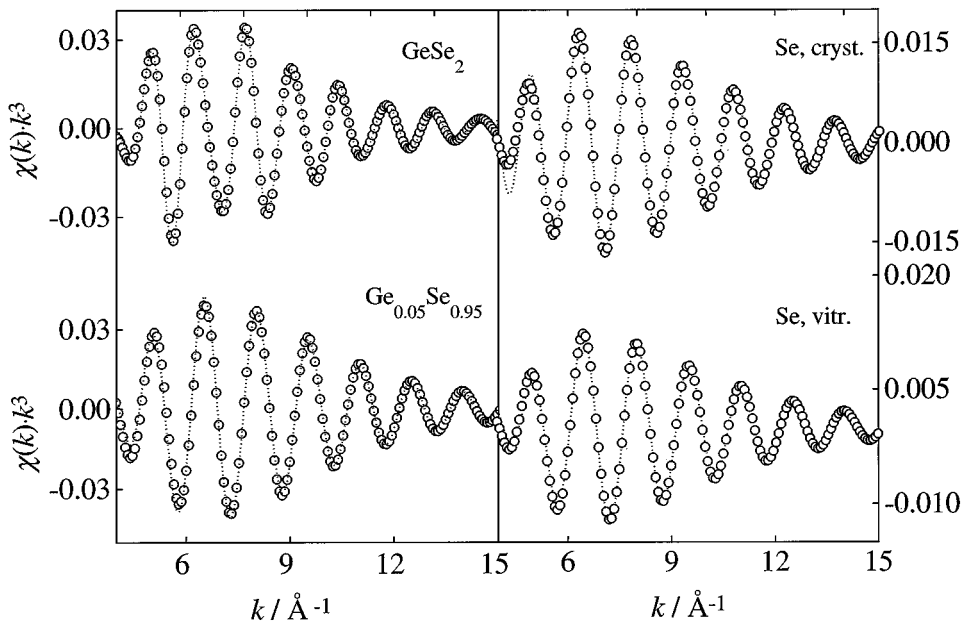


**FIG. 4.** Observed and calculated first shell EXAFS spectra: Ge K-edge data for vitreous $GeSe_2$ and $Ge_{0.05}Se_{0.95}$ (left-hand side) and Se K-edge data for crystalline and vitreous Se.

fraction Se, the corresponding increase in bond length is limited. Also for the photostructural changes reported by Gladden *et al.* (6, 7) the bond length remained approximately constant.

The results first obtained from experiments performed at SRS were not expected. Further experiments were performed at NSLS on freshly synthesized samples that never were exposed to light and to samples covered by black paper to avoid photostructural changes as well as to the samples previously studied at SRS. These experiments gave essentially the same results. Thus the results are not directly due to experimental errors and the unexpected results, if erroneous, must relate to poor sample quality or inadequate data analysis. The samples appear homogeneous by optical microscopy and amorphous by spectroscopy and diffraction. This indicates that the samples are of good quality.

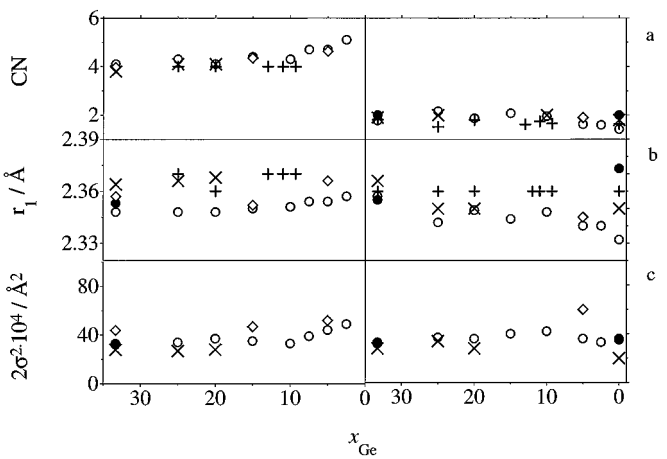


**FIG. 5.** Deduced structural data for the first coordination spheres for the Ge (left-hand side) and Se K-edges. The coordination number (a), the interatomic distance (b), and the Debye–Waller factor (c) are given as a function of composition. Circles = present results from SRS (open symbols = vitreous samples; filled symbols = crystalline samples); diamond = present results from NSLS; $x$ = Zhou *et al.* (2); + = Peyroutou *et al.* (19, 20).

A closer discussion of our spectra and our data analysis is presented. The-Ge K-edge EXAFS spectra of vitreous $GeSe_2$ and of $Ge_{0.20}Se_{0.80}$ are given in Fig. 6a. The periodicity of the spectra remains unchanged; hence, the bond length does not change. The EXAFS amplitude is damped for $Ge_{0.20}Se_{0.80}$ at high $k$ values and, hence, indicate a higher Debye–Waller factor. The coordination number is the same in both samples as seen by the amplitude in the low $k$ range of the spectra. A corresponding comparison of vitreous $GeSe_2$ and $Ge_{0.025}Se_{0.975}$ is given in Fig. 6b. Analysis of the $Ge_{0.025}Se_{0.975}$ spectrum indicates both a higher coordination number and a higher Debye–Waller factor than those obtained for $GeSe_2$. The higher coordination number gives an expanded EXAFS signal in the low $k$ range, whereas the higher Debye–Waller factor gives a damped EXAFS signal for high $k$ values. This is further illustrated in Fig. 7 where the ratio method (11, 12) has been applied to the Fourier-filtered Ge K-edge EXAFS spectra of $Ge_{0.075}Se_{0.925}$ and $Ge_{0.025}Se_{0.975}$. The logarithm of the ratio of the

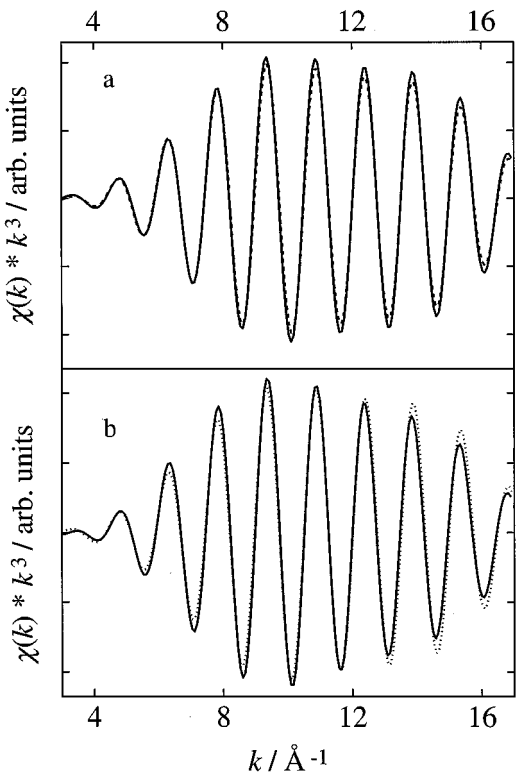


**FIG. 6.** The Ge K-edge EXAFS of (a) vitreous $GeSe_2$ (solid line) and $Ge_{0.20}Se_{0.80}$ (dotted line) and (b) vitreous $GeSe_2$ (dotted line) and $Ge_{0.025}Se_{0.975}$ (solid line).

amplitudes of the sample to the model compound is plotted against $k^2$ since

$$\ln(\chi/\chi_{\text{model}}) = \ln[\mathrm{N}\cdot r^2_{\text{model}}/(N_{\text{model}}\cdot r^2)] - 2k^2\cdot(\sigma^2 - \sigma^2_{\text{model}}).$$

Such a plot should yield a straight line if amplitude function transferability between the sample and model compound is obeyed (11,12). Vitreous $GeSe_2$ was used as the model because the structure of the glass is expected to resemble the short-range order in this compound where the coordination number is 4. The experimental curves show a linear trend down to about $k \approx 6\,\text{Å}^{-1}$. The changes in coordination number and the Debye–Waller factor are obtained from the $y$ axis intercept and from the slopes of the fitted straight lines in Fig. 7. Analysis of the data gives coordination numbers 4.8 and 4.6 for $x_{\text{Se}} = 0.975$ and 0.925, respectively. These results are in good agreement with the results from EXCURV92. Also the shift in the Debye–Waller factor is in good agreement. The ratio curves deviate from linearity only for $k$ values below $6\,\text{Å}^{-1}$. This effect may relate to errors in background subtraction or to effects from second coordination shell atoms.

Three factors may give rise to systematic errors; the use of the same model compound over an extended compositional region, multiple scattering, and anisotropic disorder. These effects are briefly considered below.

$GeSe_2$ should be a reasonable model compound for the amplitude function and reduction factor since Ge appear to be tetrahedrally coordinated in the whole compositional region. The amplitude reduction factor and the amplitude function depend also on the electronic properties of the compound studied (11). Compositional changes in the electronic properties of $Ge_{1-x}Se_x$ do occur since the $GeSe_2$ glass is reddish and transparent while glassy Se is metallic in appearance. Accordingly, a violation of amplitude transferability can not be ruled out. Still, both compounds must be categorized as semiconductors. Neither of the samples are far from a transition to a metallic state (21, 23).

Multiple scattering is only important for linear molecules and for the second or higher coordination shells (11, 12) and is not known to pollute first shell data (14). Analyses performed including multiple scattering in EXCURV92 did not affect the resulting structural parameters significantly.

Largely disordered systems often have asymmetric pair distribution functions that affect the calculated Debye–Waller factors. Such a large disorder, hence, might lead to nontransferability of phase and amplitude between a crystalline model compound and a glass. The Debye–Waller

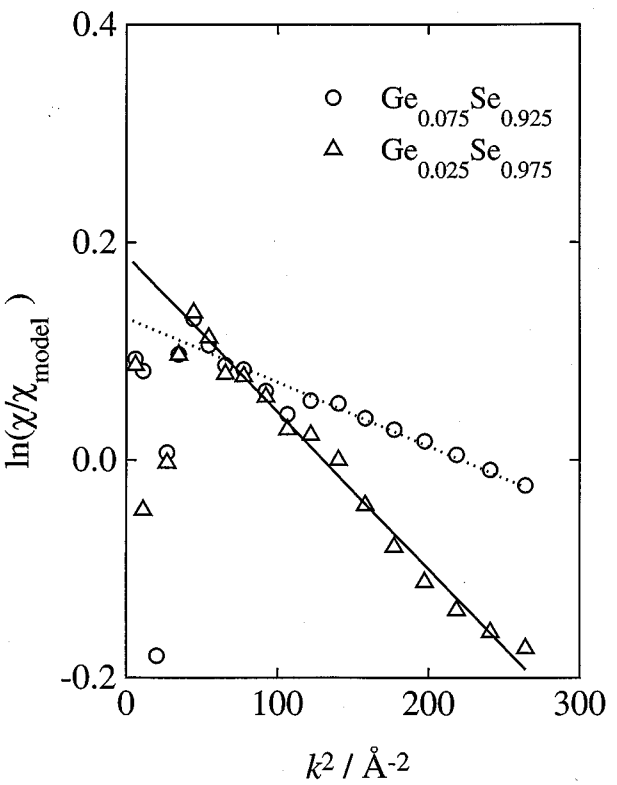


**FIG. 7.** The logarithm of the ratio of the amplitudes of $Ge_{0.075}Se_{0.925}$ (○) and of $Ge_{0.025}Se_{0.975}$ (△) to the model compound $GeSe_2$ plotted against $k^2$.

factors obtained presently, $\sigma \approx 0.05$ Å, are low compared to what is observed for systems denoted as largely disordered, $\sigma \approx 0.10$ Å (11). Adding anisotropic terms in the EXCURV92 analysis did not improve the fit between experiments and theoretical spectra. Furthermore, essentially similar structural parameters were obtained for crystalline and vitreous $GeSe_2$. This indicates that disorder is not a major source of error.

In conclusion, the $GeSe_4$ tetahedra is the main structural entity for all compositions of glassy $Ge_{1-x}Se_x$ (with $2/3 < x < 1$). This is in agreement with recent neutron diffraction (24, 25), X-ray diffraction (26), X-ray emission (27), X-ray photoelectron spectroscopy (28), and Raman scattering (3, 8) studies. A similar short-range order is also suggested for the related Ge–S system (29). Our results however also indicate slight changes in coordination with composition. These changes in SRO apparently are due to real changes in the structure of the glasses and not due to artifacts of the data analysis. We are presently not able to give a physical interpretation of the observed structural changes. We are, however, inclined to believe that these changes might relate to the effect of band-gap illumination. Overcoordination of Ge and undercoordination of Se in amorphous $GeSe_2$ illuminated by ultraviolet light have been reported by Gladden *et al.* (6, 7). The structural change in that case is due to the formation of Ge with higher coordination with terminal Se.

## ACKNOWLEDGMENTS

The authors are grateful for beamtime at SRS and NSLS. The assistance of the following persons is acknowledged: K.-C. Cheung, station scientist at station 7.1. SRS, G. Lamble at BL X11A and J. Woicik at BL X23A2 at NSLS; Ole Henrik Hansteen (University of Oslo) for assisting in the EXAFS experiments at SRS; and Claus Jørgen Nielsen (University of Oslo) for recording the Raman spectra. This work was supported by Norges Forskningsråd.

## REFERENCES

1. G. Dittmar and H. Schafer, *Acta Cryst. B* **31,** 2060 (1975).
2. W. Zhou, M. Paesler, and D. E. Sayers, *Phys. Rev. B* **43,** 2315 (1991).
3. P. Tronc, M. Bensoussan, A. Brenac, and C. Sebenne, *Phys. Rev. B* **8, 5947 (**1973).
4. R. J. Nemanich, S. A. Solin, and G. Lucovsky, *Solid State Commun.* **21,** 273 (1977).
5. P. M. Bridenbaugh, G. P. Espinosa, J. E. Griffiths, J. C. Phillips, and J. P. Remeika, *Phys. Rev. B* **20,** 4140 (1979).
6. L. F. Gladden, S. R. Elliott, G. N. Greaves, S. Cummings, and T. Rayment, *J. Non.-Cryst. Solids* **77,** 1199 (1985).
7. L. F. Gladden, S. R. Elliott, and G. N. Greaves, *J. Non-Cryst. Solids* **106,** 189 (1988).
8. S. Sugai, *Phys. Rev. B* **35,** 1345 (1987).
9. S. Stølen, H. B. Johnsen, C. Bøe, T. Grande, and O. B. Karlsen, *J. Phase Equil.* **20,** 17 (1999).
10. S. M. Heald, *in* "X-Ray Absorption: Principles, Applications, Techniques of EXAFS, SEXAFS and XANES" (D. C. Koningsberger and R. Prius, Eds.), pp. 87–118. Wiley, New York, 1988.
11. B. K. Teo, "EXAFS: Basic Principles and Data Analysis," Springer-Verlag, Berlin, 1986.
12. D. E. Sayers and B. A. Bunker, *in* "X-Ray Absorption: Principles, Applications, Techniques of EXAFS, SEXAFS and XANES" (D. C. Koningsberger and R. Prius, Eds.), pp. 211–253, Wiley, New York, 1988.
13. N. Binsted, J. W. Campbell, S. J. Gurman, and P. C. Stephenson, SERC Daresbury Laboratory EXCURV92 program, 1991.
14. M. Vaarkamp, I. Dring, R. J. Oldman, E. A. Stern, and D. C. Koningsberger, *Phys. Rev. B* **50,** 7872 (1994).
15. M. Straumanis, *Z. Kristallogr.* **102,** 432 (1940).
16. S. J. Gurman, N. Binsted, and I. Ross, *J. Phys. C*: *Solid State Phys.* **17,** 143 (1984).
17. S. J. Gurman, N. Binsted, and I. Ross, *J. Phys. C*: *Solid State Phys.* **19,** 1845 (1986).
18. F. W. H. Kampers, C. W. R. Engelen, J. H. C. van Hooff, and D. C. Koningsberger, *J. Phys. Chem.* **94,** 8574 (1990).
19. C. Peyroutou, S. Peytavin, M. Ribes, and H. Dexpert, *J. Solid State Chem.* **82,** 70 (1989).
20. C. Peyroutou, S. Peytavin, M. Ribes, and H. Dexpert, *J. Solid State Chem.* **82,** 78 (1989).
21. W. W. Warren, Jr. and R. Dupree, *Phys. Rev. B* **22,** 2257 (1980).
22. F. Shimojo, K. Hoshino, M. Watanabe, and Y. Zempo, *J. Phys.: Condens. Matter* **10,** 1199 (1998).
23. H. Krebs and R. W. Haisty, *J. Non-Cryst. Solids* **1,** 427 (1969).
24. K. Maruyama, M. Inui, S. Takeda, S. Tamaki, and Y. Kawakita, *Physica B* **213–214,** 558 (1995).
25. N. Ramesh Rao, P. S. R. Krishna, S. Basu, B. A. Dasannacharya, K. S. Sangunni, and E. S. R. Gopal, *J. Non-Cryst. Solids* **240,** 221 (1998).
26. M. M. Hafiz, F. H. Ammad, and N. A. El-Kabany, *Physica B* **183,** 392 (1993).
27. S. B. Mamedov, N. D. Aksenov, L. L. Makarov, and Yu. F. Batrakov, *J. Non-Cryst. Solids* **195,** 272 (1996).
28. M. L. Theye, A. Gheorghiu, C. Senemaud, M. F. Kotkata, and K. M. Kandil, *Philos. Mag. B* **69,** 209 (1994).
29. N. Fueki, T. Usuki, S. Tamaki, H. Okazaki, and Y. Waseda, *J. Phys. Soc. Jpn.* **61,** 2814 (1992).